

Finite-temperature magnetism of transition metals: an LDA+DMFT approach.

A. I. Lichtenstein and M. I. Katsnelson*

University of Nijmegen, NL-6525 ED Nijmegen, The Netherlands

G. Kotliar

Serin Physics Laboratory, Rutgers University, Piscataway, New Jersey 08855

(June 26, 2021)

We present an *ab initio* quantum theory of the finite temperature magnetism of iron and nickel. A recently developed technique which combines dynamical mean-field theory with realistic electronic structure methods, successfully describes the many-body features of the one electron spectra and the observed magnetic moments below and above the Curie temperature.

The theory of itinerant electron ferromagnetism is one of the central problems in condensed matter physics (for reviews see [1,2]). There is a need for a first principles approach which is able to describe ground state and thermodynamical quantities, as well as the one particle spectral properties of itinerant magnets. These quantities are currently being probed in spin polarized tunneling as well as spin polarized photoemission experiments with a view to possible applications as spin valves [3].

Iron and nickel are the oldest and experimentally best studied prototypical systems, and serve as benchmarks for electronic structure methods. At very low temperatures, a band like description of Fe and Ni has been very successful. The density functional theory (DFT) in the local density approximations (LDA) gives a quantitatively accurate description of several ground state properties of these materials such as the ordered magnetic moment and the spin wave stiffness [4] as calculated from the spin wave dispersion.

While density functional theory, can in principle provide a rigorous description of the finite temperature thermodynamic properties, at present there is no accurate practical implementation available. As a result the finite temperature properties of magnetic materials are estimated following a simple suggestion [5], whereby constrained DFT at $T=0$ is used to extract exchange constants for a *classical* Heisenberg model, which in turn is solved using approximation methods (e.g. RPA, mean field) from classical statistical mechanics of spin systems [5–8]. The most recent implementation of this approach gives good values for the transition temperature of iron but not of nickel [9]. While these localized spin models give, by construction, at high temperatures a Curie-Weiss like magnetic susceptibility, as observed experimentally in Fe and Ni, they encountered difficulties in predicting the correct values of the Curie constants [10].

It has been recognized for a long time, that to describe the finite temperature aspects of itinerant electron magnets, one needs a formalism that takes into account the existence of local magnetic moments present

above T_C [11,12]. This one of the central problems in the physics of strongly correlated electron systems, which forces us to reconcile the dual character of the electron, which as a particle requires a real space description and as a wave requires a momentum space description in a unified framework. A very successful method satisfying these requirements, the dynamical mean-field theory (DMFT) [13], has been recently developed. This many-body scheme can be combined with standard LDA band structure calculations to include the effects of a realistic band structure [14,15]. Such “LDA+DMFT” approach has been successfully applied for the computations of electronic structure and spin-wave spectrum of iron [16,17]. Nevertheless the most difficult and interesting finite-temperature effects were not considered previously and are the subject of this letter.

Here we present realistic LDA+DMFT calculations of finite temperature magnetic properties of iron and nickel. A numerically exact Quantum Monte-Carlo (QMC) scheme is used for the solution the DMFT equations. We find that a consistent first principles description of the magnetic properties and of the one electron spectra of iron and nickel is possible, within an approach that makes only two essential approximations: the locality of the electron self energy and of the particle hole irreducible vertex [13].

There have been numerous efforts to construct a many body theory of these materials, for example using the T-matrix theory [18], a self-consistent moment method [19], local 3-body equations [20,21] and the GW [22] approximations. The LDA+DMFT approach goes beyond these works in the treatment of a realistic orbitally degenerate band structure, and in the treatment of the many body interactions.

We start with the LDA Hamiltonian in the tight-binding orthogonal LMTO representation $H_{mm'}^{LDA}(\mathbf{k})$ [23], where m describes the orbital basis set containing $3d$ -, $4s$ - and $4p$ - states. \mathbf{k} runs over the Brillouin zone (BZ). The interactions are parameterized by a matrix of screened local Coulomb interactions $U_{mm'}$ and a matrix of

exchange constants $J_{mm'}$, which are expressed in terms of two screened Hubbard parameters U and J , describing the average Coulomb repulsion and the interatomic ferromagnetic exchange respectively. We use the values $U = 2, 3$ (3, 0) eV for Fe (Ni) and the same value of the interatomic exchange, $J = 0.9$ eV for both Fe and Ni, a result of constrained LDA calculations [24,14,15].

Dynamical mean-field theory maps the many-body system onto a multi-orbital quantum impurity, i.e. a set of local degrees of freedom in a bath described by the Weiss field function \mathcal{G} . The impurity action (here $n_{m\sigma} = c_{m\sigma}^\dagger c_{m\sigma}$ and $\mathbf{c}(\tau) = [c_{m\sigma}(\tau)]$ is a vector of Grassman variables) is given by:

$$S_{eff} = \int_0^\beta d\tau \int_0^\beta d\tau' Tr[\mathbf{c}^+(\tau) \mathcal{G}^{-1}(\tau, \tau') \mathbf{c}(\tau')] + \quad (1)$$

$$\frac{1}{2} \sum_{m,m',\sigma} \int_0^\beta d\tau [U_{mm'} n_\sigma^m n_{-\sigma}^{m'} + (U_{mm'} - J_{mm'}) n_\sigma^m n_\sigma^{m'}]$$

It describes the spin, orbital, energy and temperature dependent interactions of particular magnetic $3d$ -atom with the rest of the crystal and is used to compute the local Greens function matrix:

$$\mathbf{G}_\sigma(\tau - \tau') = -\frac{1}{Z} \int D[\mathbf{c}, \mathbf{c}^+] e^{-S_{eff}} \mathbf{c}(\tau) \mathbf{c}^+(\tau') \quad (2)$$

(Z is the partition function) and the impurity self energy $\mathcal{G}_\sigma^{-1}(\omega_n) - \mathbf{G}_\sigma^{-1}(\omega_n) = \Sigma_\sigma(\omega_n)$.

The Weiss field function is required to obey the self consistency condition [14,15], which restores translational invariance to the impurity model description:

$$\mathbf{G}_\sigma(\omega_n) = \sum_{\mathbf{k}} [(i\omega_n + \mu)\mathbf{1} - \mathbf{H}^{LDA}(\mathbf{k}) - \Sigma_\sigma^{dc}(\omega_n)]^{-1} \quad (3)$$

μ is the chemical potential defined self-consistently through the total number of electrons, $\omega_n = (2n + 1)\pi T$ are the Matsubara frequencies for temperature $T \equiv \beta^{-1}$ ($n = 0, \pm 1, \dots$) and σ is the spin index. The local matrix Σ_σ^{dc} is the sum of two terms, the impurity self energy and a so-called “double counting” correction, E_{dc} which is meant to subtract the average electron-electron interactions already included in the LDA Hamiltonian. For metallic systems we propose the general form of dc-correction: $\Sigma_\sigma^{dc}(\omega) = \Sigma_\sigma(\omega) - \frac{1}{2} Tr_\sigma \Sigma_\sigma(0)$. This is motivated by the fact that the static part of the correlation effects are already well described in the density functional theory. Only the d -part of the self-energy is presented in our calculations, therefore $\Sigma_\sigma^{dc} = 0$ for s - and p - states as well as for non-diagonal $d-s, p$ contributions. In order to describe the finite temperature ferromagnetism of transition metals we use the *non* spin-polarized LDA Hamiltonian $\mathbf{H}^{LDA}(\mathbf{k})$ and accumulate *all* temperature-dependent spin-splittings in the self-energy matrix $\Sigma_\sigma^{dc}(\omega_n)$.

We use the impurity QMC scheme for the solution of the multiband DMFT equations [25]. The Hirsch discrete Hubbard-Stratonovich transformations introduces

$(2M - 1)M$ auxiliary Ising fields $S_{mm'}^{\sigma\sigma'}$, where M is the orbital degeneracy of the d -states and calculate $\mathbf{G}_\sigma(\tau)$ by an exact integration of the fermion degrees of freedom in the functional integral (Eq.(2)) [13]. In order to sample efficiently all the spin configurations in the multi-band QMC scheme, it is important to use “global” spin-flips: $[S_{mm'}^{\sigma\sigma'}] \rightarrow [-S_{mm'}^{\sigma-\sigma'}]$ in addition to the local moves of the auxiliary fields. The number of QMC sweeps was of the order of 10^5 . A parallel version of the DMFT program was used to sample the 45 Ising fields for $3d$ -orbitals. We used 256 \mathbf{k} -points in the irreducible part of the BZ for the \mathbf{k} integration. 10 to 20 DMFT iterations were sufficient to achieve convergence far from the Curie point. Due to the cubic symmetry of the bcc-Fe and fcc-Ni lattices the local Green function is diagonal in the basis of real spherical harmonics. The spectral functions for real frequencies were obtained from the QMC data by applying the maximum entropy method [26].

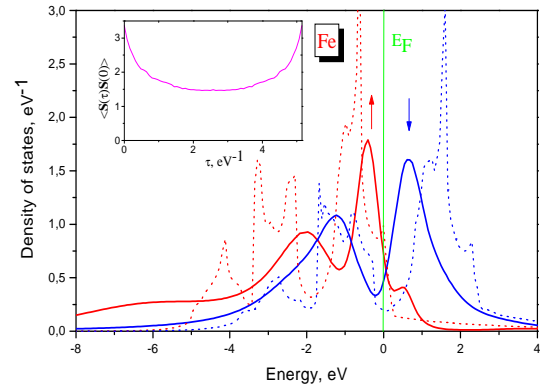


FIG. 1. LDA+DMFT results for ferromagnetic iron ($T = 0.8 T_C$). The partial densities of d -states (full lines) is compared with the corresponding LSDA results at zero temperature (dashed lines) for the spin-up (red lines, arrow-up) and spin-down (blue lines, arrow-down) states. The insert shows the spin-spin autocorrelation function for $T = 1.2 T_C$.

Our results for the local spectral function for iron and nickel are shown in Figs.1 and 2, respectively. The LDA+DMFT approach describes well all the qualitative features of the density of states (DOS), which is especially non-trivial for nickel. Our QMC results reproduce well the three main correlation effects on the one particle spectra below T_C [27]: the presence of a famous 6 eV satellite, the 30% narrowing of the occupied part of d -band and the 50% decrease of exchange splittings compared to the LDA results. Note that the satellite in Ni has substantially more spin-up contributions in agreement with photoemission spectra [27]. Correlation effects in Fe are less pronounced than in Ni, due to its large spin-splitting and the characteristic bcc-structural dip in the density of states for spin-down states near Fermi level, which reduces the density of states for particle hole excitations.

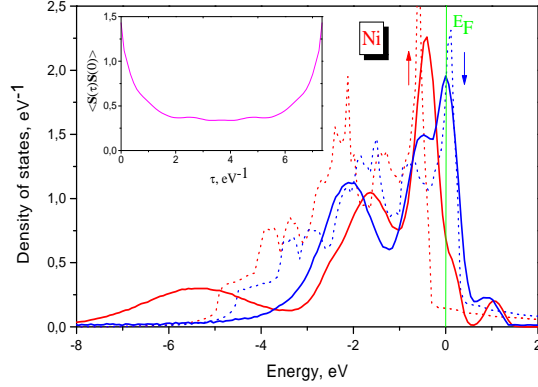


FIG. 2. Same quantities as in Fig.1 for ferromagnetic nickel ($T = 0.9 T_C$). The insert shows the spin-spin autocorrelation function for $T = 1.8 T_C$.

The uniform spin susceptibility in the paramagnetic state:

$$\chi_{q=0} = \frac{dM}{dH} \quad (4)$$

was extracted from the QMC simulations by measuring the induced magnetic moment in a small external magnetic field. It includes the polarization of the impurity Weiss field by the external field [13].

The dynamical mean field results accounts for the observed Curie -Weiss law which is observed experimentally in Fe and Ni. As the temperature increases above T_C , the atomic character of the system is partially restored resulting in an atomic like susceptibility with an effective moment:

$$\chi_{q=0} = \frac{\mu_{eff}^2}{3(T - T_C)} \quad (5)$$

The temperature dependence of the ordered magnetic moment below the Curie temperature and the inverse of the uniform susceptibility above the Curie point are plotted in Fig. 3 together with the corresponding experimental data for iron and nickel [28,1]. The LDA+DMFT calculations describes the magnetization curve and the slope of the high-temperature Curie-Weiss susceptibility remarkably well. The calculated values of high-temperature magnetic moments extracted from Eq.(4) are $\mu_{eff} = 3.09$ (1.50) μ_B for Fe (Ni), in good agreement with the experimental data $\mu_{eff} = 3.13$ (1.62) μ_B for Fe (Ni) [28].

We have estimated the values of the Curie temperatures of Fe and Ni from the disappearance of spin polarization in the self-consistent solution of DMFT problem and from the Curie-Weiss law in (Eq.(5)). Our estimates $T_C = 1900$ (700) K are in reasonable agreement with experimental values of 1043 (631) K for Fe (Ni) respectively [28], considering the single site nature of the DMFT approach.

Within dynamical mean field theory one can also compute the local spin susceptibility defined by

$$\chi_{loc} = \frac{g_s^2}{3} \int_0^\beta d\tau \langle \mathbf{S}(\tau) \mathbf{S}(0) \rangle \quad (6)$$

where $g_s = 2$ is the gyromagnetic ratio and $\mathbf{S} = \frac{1}{2} \sum_{m,\sigma,\sigma'} c_{m\sigma}^\dagger \boldsymbol{\sigma}_{\sigma\sigma'} c_{m\sigma'}$ is single-site spin operator and $\boldsymbol{\sigma} = (\sigma_x, \sigma_y, \sigma_z)$ are Pauli matrices. It differs from the $q = 0$ susceptibility, Eq.(4), by the absence of spin polarization in the Weiss field of the impurity model. Eq.(6) cannot be probed directly in experiments but it is easily computed in DMFT-QMC. Its behavior as function of temperature, gives a very intuitive picture of the degree of correlations in the system. In a weakly correlated system we expect Eq.(6) to be nearly temperature independent, while in a strongly correlated system we expect a leading Curie-Weiss behavior at high temperatures $\chi_{local} = \mu_{loc}^2 / (3T + const)$ where μ_{loc} is an effective local magnetic moment. In the Heisenberg model with spin S , $\mu_{loc}^2 = S(S+1)g_s^2$ and for well-defined local magnetic moments (e.g., for rare earth magnets) this quantity should be temperature independent. For the itinerant electron magnets μ_{loc} is temperature-dependent, due to a variety of competing many body effects such as Kondo screening, the induction of local magnetic moment by temperature [12] and thermal fluctuations which disorders the moments [29]. All these effects are included in the DMFT calculations. The τ -dependence of the correlation function $\langle \mathbf{S}(\tau) \mathbf{S}(0) \rangle$ results in the temperature dependence of μ_{loc} and is displayed in the inserts on the Figs.1,2. Iron can be considered as a magnet with very well-defined local moments above T_C (the τ -dependence of the correlation function is relatively weak), whereas nickel is more itinerant electron magnet (stronger τ -dependence of the local spin-spin autocorrelation function).

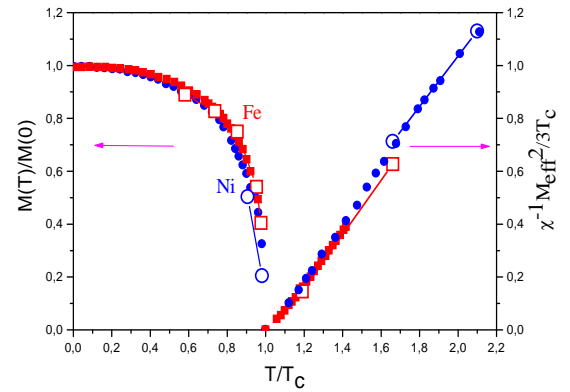


FIG. 3. Temperature dependence of ordered moment and the inverse ferromagnetic susceptibility for Fe (open square) and Ni (open circle) compared with experimental results for Fe (square) and Ni (circle) (from Ref.[1,28]).

The comparison of the values of the local and the $q = 0$ susceptibility gives a crude measure of the degree of short range order which is present above T_C . As expected, the moments extracted from the local susceptibility Eq.(6) are a bit smaller ($2.8 \mu_B$ for iron and $1.3 \mu_B$ for nickel) than those extracted from the uniform magnetic susceptibility. This reflects the small degree of the short-range correlations which remain well above T_C [30]. The high-temperature LDA+DMFT clearly show the presence of a local-moment above T_C . This moment, is correlated with the presence of high energy features (of the order of the Coulomb energies) in the photoemission. This is also true below T_C , where the spin dependence of the spectra is more pronounced for the satellite region in nickel than for that the quasiparticle bands near the Fermi level (Fig. 2). This can explain the apparent discrepancies between different experimental determinations of the high-temperature magnetic splittings [11,31,32] as being the result of probing different energy regions. The resonant photoemission experiments [31] reflects the presence of local-moment polarization in the high-energy spectrum above Curie temperature in nickel, while the low-energy ARPES investigations [32] results in non-magnetic bands near the Fermi level. This is exactly the DMFT view on the electronic structure of transition metals above T_C . Fluctuating moments and atomic-like configurations are large at short times, which results in correlation effects in the high-energy spectra such as spin-multiplet splittings. The moment is reduced at longer time scales, corresponding to a more band-like, less correlated electronic structure near the Fermi level.

To conclude, we presented the first results of *ab initio* LDA+DMFT calculations of finite-temperature magnetic properties for Fe and Ni and showed that many body effects which incorporate the local atomic character of the electrons and which are ignored in the standard LDA based scheme are essential for a simultaneous description of the magnetic properties and the one electron spectra of itinerant electron magnets. DMFT gives a satisfactory semiquantitative description of the physical properties of Fe and Ni, far from the Curie point, indicating that the critical fluctuations, which are not included in the DMFT approximation, do not play a crucial role, except for the immediate vicinity of the transition, and many aspects of the physics of this system can be understood within an approach which stresses local physics. It would be interesting to extend this study to other itinerant magnetic systems with more atoms per unit cell, such as SrRuO_3 which is also well described by band theory at very low temperatures but has anomalous properties above its Curie point [33].

ACKNOWLEDGEMENT This work is supported by the Netherlands Organization for Scientific Research, grant NWO 047-008-16. GK was supported by the ONR, grant No. 4-2650. A.I.L. is grateful to the Center for Materials Theory at Rutgers University for its hospitality, during the initial stages of this work.

-
- * Permanent address: Institute of Metal Physics, Ekaterinburg 620219, Russia.
- [1] S. V. Vonsovsky, *Magnetism*, vol.2 (John Wiley, N.Y., 1974).
 - [2] D. Vollhardt *et al.*, *Advances In Solid State Physics*, **38**, p. 383 (Vieweg, Wiesbaden 1999)
 - [3] Slouten R. J. *et al*, *Science*, **282**, 85 (1998).
 - [4] S.Y. Savrasov, *Phys. Rev. Lett.* **81**, 2570 (1998).
 - [5] A.I. Liechtenstein *et al.*, *J. Magn. Magn. Mat.* **67**, 65 (1987).
 - [6] N. M. Rosengaard and B. Johansson, *Phys. Rev. B* **55**, 14975 (1997).
 - [7] S. V. Halilov *et al.*, *Phys. Rev. B* **58**, 293 (1998).
 - [8] V. P. Antropov, *et al.*, *Phys. Rev. B* **54**, 1019 (1996).
 - [9] M. Pajda *et al.*, cond-mat 0007441
 - [10] J. B. Staunton and B. L. Gyorffy, *Phys. Rev. Lett.* **69**, 371 (1992).
 - [11] E. Kisker *et al.*, *Phys. Rev. Lett.* **52**, 2285 (1984); A. Kakizaki *et al*, *Phys. Rev. Lett.* **72**, 2781 (1994).
 - [12] T. Moriya, *Spin Fluctuations in Itinerant Electron Magnetism* (Springer, Berlin etc., 1985).
 - [13] For a review see: A. Georges *et al.*, *Rev. Mod. Phys.* **68**, 13 (1996).
 - [14] V.I. Anisimov *et al.*, *J. Phys.: Cond. Matt.* **9**, 7359 (1997).
 - [15] A. I. Lichtenstein and M. I. Katsnelson, *Phys. Rev. B* **57**, 6884 (1998).
 - [16] M. I. Katsnelson and A. I. Lichtenstein, *J. Phys.: Cond. Matt.* **11**, 1037 (1999).
 - [17] M. I. Katsnelson and A. I. Lichtenstein, *Phys. Rev. B* **61**, 8906 (2000).
 - [18] A. Liebsch, *Phys. Rev. Lett.* **43**, 1431 (1979).
 - [19] W. Nolting, *et al*, *Phys. Rev. B* **40**, 5015 (1989).
 - [20] J. Igarashi *et al*, *Phys. Rev. B* **49**, 16181 (1994).
 - [21] F. Manghi *et al*, *Phys. Rev. B* **59**, R10409 (1999).
 - [22] F. Aryasetiawan, *Phys. Rev. B* **46**, 13051 (1992).
 - [23] O.K. Andersen and O. Jepsen, *Phys. Rev. Lett.* **53**, 2571 (1984).
 - [24] T. Bandyopadhyay and D.D. Sarma, *Phys. Rev. B* **39**, 3517 (1989).
 - [25] M. J. Rozenberg, *Phys. Rev. B* **55**, R4855, (1997).
 - [26] M. Jarrell and J. E. Gubernatis, *Physics Reports* **269**, 133 (1996).
 - [27] See, e.g., recent work K. N. Altmann *et al.*, *Phys. Rev. B* **61**, 15661 (2000) and refs. therein.
 - [28] *Ferromagnetic materials*, vol. 1, ed. by E.P. Wolfarth (North-Holland, Amsterdam, 1986).
 - [29] V. Yu. Irkhin and M. I. Katsnelson, *Physics - Uspekhi* **37**, 659 (1994).
 - [30] H.A. Mook and J.W. Lynn, *J. Appl. Phys.* **57**, 3006 (1985).
 - [31] B. Sinković *et al.*, *Phys. Rev. Lett.* **79**, 3510 (1997).
 - [32] T. J. Kreutz *et al.*, *Phys. Rev. B* **58**, 1300 (1998).
 - [33] J. S. Dodge *et al.*, cond-mat/0006271.